ELSEVIER

Energy and Buildings 33 (2001) 613–625

ENERGY AND BUILDINGS

www.elsevier.com/locate/enbuild

A two-layer turbulence model for simulating indoor airflow Part I. Model development

Weiran Xu, Qingyan Chen*

Department of Architecture, Massachusetts Institute of Technology, 77 Massachusetts Avenue, MA 02139, USA

Received 2 August 2000; accepted 7 October 2000

Abstract

Energy efficient buildings should provide a thermally comfortable and healthy indoor environment. Most indoor airflows involve combined forced and natural convection (mixed convection). In order to simulate the flows accurately and efficiently, this paper proposes a two-layer turbulence model for predicting forced, natural and mixed convection. The model combines a near-wall one-equation model [J. Fluid Eng. 115 (1993) 196] and a near-wall natural convection model [Int. J. Heat Mass Transfer 41 (1998) 3161] with the aid of direct numerical simulation (DNS) data [Int. J. Heat Fluid Flow 18 (1997) 88]. © 2001 Published by Elsevier Science B.V.

Keywords: Two-layer turbulence model; Low-Reynolds-number (LRN); k–ε Model (KEM)

1. Introduction

1.1. Objectives

Energy efficient buildings should provide a thermally comfortable and healthy indoor environment. The comfort and health parameters in indoor environment include the distributions of velocity, air temperature, relative humidity, and contaminant concentrations. These parameters can be obtained by using the computational fluid dynamics (CFD). On the other hand, indoor airflow have the impact on building energy consumption. For example, it is well-known that displacement ventilation can save energy because of the temperature stratification in a room. In addition, different flow patterns can result in very different heat transfer coefficients on building enclosures. The corresponding heat gain and loss will not be the same.

Many indoor airfiows involve all three types of convection: forced, natural and mixed convection. Accurate simulation of these flows is essential for building ventilation system design. The CFD simulations often use turbulence models, since most flows encountered indoors are turbulent. However, the existing turbulence models are either inaccurate, such as the standard k–ε model (KEM), or inefficient, such as low-Reynolds-number (LRN) KEMs and Reynolds stress models (RSMs), to predict all three types of convection. This paper presents a new two-layer turbulence model that performs two tasks:

1. It can accurately predict flows under various conditions, i.e. from purely forced to purely natural convection. This model allows building ventilation designers to use one single model to calculate flows instead of selecting different turbulence models empirically from many available models.
2. It can be more efficient than available turbulence models, such as LRN models and RSMs.

1.2. Earlier work

Purely forced and natural convection can be viewed as two extreme cases of mixed convection. Mixed convection is more complicated than forced convection and natural convection since it combines the complexity of both. Turbulent forced convection has been extensively studied and most turbulence models are developed for forced flows. A review of the studies on turbulent natural convection can be found in [2]. This section reviews the state-of-the-art studies of turbulent mixed convection and identifies the problems with the existing turbulence models.

Studies on turbulent mixed convection fall into three categories: theoretical analysis, experimental investigation and numerical simulation. Theoretical studies include those by Nakajima and Fukui [4], Chen et al. [5] and Aicher and Martin [6]. Nakajima and Fukui [4] and Chen et al. [5]

* Corresponding author.

0378-7788/01/$ – see front matter © 2001 Published by Elsevier Science B.V.
PII: S0378-7788(00)00129-8

Nomenclature

A_μ, A_ε	constants used in the one-equation models
Ar_b	bulk Archimedes number, $g\beta\Delta TL/U_{bulk}^2$
Ar_y	local Archimedes number, $g\beta\Delta T y_n/U^2$
$C_{1\varepsilon}$, $C_{2\varepsilon}$, $C_{3\varepsilon}$	constants used in the ε equation
C_μ	constant used for calculating v_t
d_k	diffusion of turbulent kinetic energy
g_i	component i of the gravitation vector
G	gravitational acceleration
G_k	gravity production of turbulent kinetic energy ($-\beta g_i\overline{u_i t}$)
Gr_x	local Grashof number ($\beta g\Delta T x^3/v^2$)
h	convective heat transfer coefficient
k	turbulent kinetic energy ($\overline{u_i u_i}/2$)
L	characteristic length
Nu_x	local Nusselt number (hx/λ_{air})
p	fluctuating pressure
P_k	shear production of the turbulent kinetic energy ($-\overline{u_i u_j}\partial U_i/\partial x_j$)
P_t	total pressure
Pr	Prandtl number
Pr_t	turbulent Prandtl number
Ra	Rayleigh number ($\beta g\Delta TL^2/v\lambda$)
Re	Reynolds number
t	fluctuating temperature or time
T	mean temperature
T_a	ambient temperature
u, v	fluctuating velocity component in x, y direction
u_i	component i of fluctuating velocity
u_τ	friction velocity, $\sqrt{\tau_w/\rho}$
$\overline{u_i u_j}$	Reynolds stress
$\overline{u_i t}$	turbulent heat flux
U_i	component i of the mean velocity
U, V, W	mean velocity component in x, y and z direction
V_c	characteristic velocity, $\sqrt{\beta g\Delta TL}$
x, y, z	spatial coordinate
y_n	normal distance to the nearest wall
y^+, y^*, y_v^*	dimensionless wall distance, $y_n u_\tau/v$, $y_n\sqrt{k}/v$, $y_n\sqrt{vv}/v$

Greek symbols

β	thermal expansion coefficient $-(1/\rho)(\partial\rho/\partial T)$
δ_{ij}	Kronecker delta
ε	turbulent energy dissipation
λ	thermal conductivity
v	molecular viscosity
v_t	turbulent viscosity
ρ	fluid density
σ_k, σ_ε	Prandtl number of k and ε
τ_w	wall shear stress

Superscript

—	time-averaged quantities
~	instantaneous quantities
+	non-dimensionlized by wall-friction quantities

Subscripts

i, j	spatial coordinate indices
nb	neighbor points
ref	reference conditions
t	turbulent quantities

independently proposed damping functions similar to Van Driest's [7] to enable the mixing-length model to count the buoyancy effects. They also conducted an experiment in a long channel to study basic turbulence and heat transfer characteristics of mixed convection. Aicher and Martin [6] proposed two heat transfer correlations for the mixed convection in a tube. These studies provided some physical insights to understand the mixed convection. For example, Nakajima and Fukui found that the heat transfer in the boundary layer of a plate was decreased when the plate was slightly heated. Aicher and Martin [6] suggested that the decrease was due to the reduction of the turbulent energy in the boundary layer.

Experimental investigations on turbulent mixed convection that can be directly used for validation of numerical simulations, i.e. those with simple geometry and boundary conditions, are very few. The only notable contributions are those by Schwenke [8] and Blay et al. [9]. Schwenke conducted a series of measurements in a ventilated room with a heated wall. He measured the penetration length, which is the length of how far the air stream from a diffuser can propagate against the buoyancy-induced wall jet. He found that the energy imposed on the heated wall had a significant impact on the airflow pattern. This case can represent the airflow in a typical ventilated room with a hot window. Blay et al. measured the mixed convection flow in a two-dimensional cavity. Their measured quantities include velocities, temperatures and velocity fluctuations at mid-width and mid-height plane of the cavity. Both studies have been selected to validate the model developed in this paper.

Numerical simulations of mixed convection are widely available in literature. Nielsen et al. [10] used the standard KEM with the wall functions and calculated the flows in a ventilated room with floor heating some 20 years ago. Though the prediction agreed reasonably with the experimental data, it is well known that the wall functions cannot calculate buoyancy effects accurately. In addition, their results do not agree well with Schwenke's experimental data [8]. In spite of these, this early attempt showed the great potential of numerical simulation and it was considered as a milestone in applying the CED technique to indoor airflow simulations.

Many other researchers have applied LRN KEMs to calculate mixed convection flows in vertical pipes [11],

vertical channels [12,13], vertical boundary layers [14], and cavities [9,15]. These computational results have been compared with the corresponding experimental data and the agreement was reasonably good. However, the computing costs in these applications were very high. For example, To and Humphrey [15] found that at least five grids are needed in the viscous sublayer and 17 in the buffer layer to produce acceptable results.

Chen [16] systematically compared the performance of several KEMs on indoor airflow simulation and found that the performance of various turbulence models was so diverse that no model can be used universally. For example, he found the RNG KEM performed best in mixed convection but very poor in forced convection flows.

Very few researchers have attempted to apply the RSMs on indoor airflow simulations. One contribution is due to Chen [17]. He found that the performance of the RSMs in mixed convection is less satisfactory than that in forced and natural convection.

So far, only one DNS study has been performed towards turbulent mixed convection [3]. This DNS was performed for fully developed channel flows with small buoyancy effects. This paper has employed their data to develop a one-equation turbulence model.

In summary, for turbulent mixed convection, few theoretical and experimental studies exist due to its complexity. Most numerical simulations on the mixed convection have employed various versions of the LRN KEMs while few others have applied the RSMs. The computing efforts required by a LRN KEM or a RSM are very high. An accurate and cost-effective turbulence model is not available. The next section describes our effort to develop such a model.

2. One-equation near-wall models for forced, natural, and mixed convection

This section develops a new one-equation near-wall turbulence model with the aid of Kasagi and Nishimura's DNS data [3]. After a briefly description of the DNS data, the paper will access the turbulent kinetic energy equation term by term. Then, we will formulate a new one-equation, near-wall model and construct a two-layer model by using the new one-equation model in the near-wall region and the standard k–ε model in the outer-wall region.

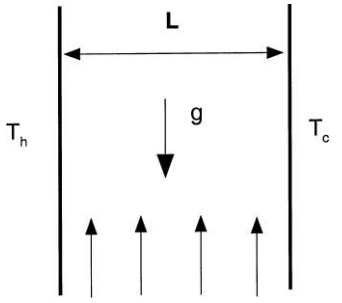

Fig. 1. The configuration used in the DNS study [3].

2.1. Brief description of the DNS data

Kasagi and Nishimura [3] conducted a DNS study for the configuration shown in Fig. 1 under various Grashof numbers. The free stream flow in the channel is heated at one side and cooled at the other.

Table 1 summarizes the flow conditions under which the DNS was performed. The table also includes the conditions for the DNS data from Versteegh and Nieuwstadt [18] as a comparison. The table shows that cases 1–4 have a similar Reynolds number while the Grashof numbers varies from 0–1.6×10^6. According to Kasagi and Nishimura [3], cases 1, 2 and 4 were performed on a relatively coarse grid ($64 \times 48 \times 64$) while case 3 on a finer grid ($128 \times 128 \times 96$). The last row of the table gives the overall Archimedes numbers, Ar_b, which is the ratio of buoyancy force and inertia force in the fluid. The Archimedes number indicates that, except for case 5, the buoyancy is weak. These data will be used in the next section to access the turbulent kinetic energy equation.

2.2. Assessment of the k-equation model

Eddy-viscosity models usually require a length scale and a velocity scale to calculate the eddy-viscosity. In one-equation turbulence models, the length scale is often prescribed while the turbulent kinetic energy, k, is often chosen as the velocity scale. k can be obtained by solving its transport equation, k-equation. The exact k-equation reads:

$$\frac{\partial k}{\partial t} + U_i \frac{\partial k}{\partial x_i} = d_k + P_k + G_k - \varepsilon \tag{1}$$

Table 1
Flow conditions of the DNS databases

Case	1	2	3	4	5
Flow type	Forced convection	Mixed convection	Mixed convection	Mixed convection	Natural convection [18]
Re_b	4358	4341	4494	4148	0
Gr_b	0.0	6.4×10^5	9.6×10^5	1.6×10^6	7.714×10^5
$Ar_b = (Gr_b/Re_b^2)$	0.0	0.0339	0.0475	0.0930	∞

where

$$d_k = \frac{\partial}{\partial x_k}\left(-\frac{\overline{u_i u_i u_k}}{2} + \frac{1}{\rho}\overline{pu_k} + \nu\frac{\partial k}{\partial x_k}\right) \tag{2}$$

represents the total diffusion contribution from turbulence, pressure, and viscous transport. The shear production term reads

$$P_k = -\overline{u_i u_j}\frac{\partial U_i}{\partial x_j} \tag{3}$$

The buoyancy production/destruction term is

$$G_k = \frac{1}{\rho}\frac{\partial \rho}{\partial T}\, g_i \overline{u_i t} \tag{4}$$

If the overheat ratio ($\Delta T/T_{\mathrm{ref}}$) is small, the Boussinesq assumption is valid and the buoyancy term can be further simplified to

$$G_k = -\beta g_i \overline{u_i t} \tag{5}$$

where g_i is the gravity vector component and β the thermal expansion coefficient. The last term of Eq. (1), denoted as ε, represents turbulence dissipation:

$$\varepsilon = \nu\,\overline{\frac{\partial u_i}{\partial x_j}\frac{\partial u_i}{\partial x_j}} \tag{6}$$

The exact k-equation, Eq. (1), introduces the following unknown quantities: $\overline{u_i u_i u_k}, \overline{pu_i}, \overline{u_i u_j}, \overline{u_i t}$ and ε. Unless additional transport equations are introduced to solve them, these quantities must be modeled. The left-hand-side of the exact k-equation is known, and it does not require modeling. The right-hand-side terms and their models are listed in Table 2. As suggested by Prandtl [19], the modeled form can be obtained by substituting the following eddy-viscosity assumptions into the exact form:

$$-\frac{1}{2}\overline{u_i u_i u_j} + \frac{1}{\rho}\overline{pu_j} = \frac{\nu_t}{\sigma_k}\frac{\partial k}{\partial x_j} \tag{7}$$

$$-\overline{u_i u_j} = \nu_t\left(\frac{\partial U_i}{\partial x_j} + \frac{\partial U_j}{\partial x_i}\right) - \frac{2}{3}\delta_{ij}k \tag{8}$$

$$-\overline{u_i t} = \frac{\nu_t}{Pr_t}\frac{\partial T}{\partial x_i} \tag{9}$$

$$\varepsilon = \frac{k^{3/2}}{l_\varepsilon} \tag{10}$$

The eddy viscosity is computed by

$$\nu_t = C_\mu \sqrt{k} l_\mu \tag{11}$$

We applied the following conditions

$$\frac{\partial}{\partial x} = 0, \qquad \frac{\partial}{\partial z} = 0 \qquad V = W = 0 \tag{12}$$

which are appropriate for the configuration shown in Fig. 1, to the modeled form of the k-equation and obtained the expanded form, as shown in Table 2.

Xu et al. [2] suggested that buoyancy could modify the budget of the turbulent kinetic energy equation. Fig. 2 shows the k-equation budget of cases 1–4. It is clear that the shear production and the dissipation terms dominate the entire boundary layer. This is quite different from what found by Xu et al. [2] in the natural convection case, where shear production only has a small contribution in the immediate near-wall region. A careful term-by-term examination of the k-equation under mixed convection is therefore necessary.

In order to conduct the term-by-term assessment, the eddy viscosity ν_t in Eqs. (7)–(9) has been evaluated by

$$\nu_t = -\frac{\overline{uv}}{(\mathrm{d}U/\mathrm{d}y)} \tag{13}$$

However, Eq. (13) shows sharp peaks due to the velocity maximum. We have smoothed the eddy viscosity by linear interpolation. An example of the smoothening process is shown in Fig. 3a. Fig. 3b depicts the smoothed ν_t. These 'polished' values will be used in the following term-by-term assessment.

The left-hand side of Eq. (1) is known and does not need modeling. The first term on the right-hand side, d_k, and its model, $(\partial/\partial y)[(\nu + (\nu_t/\sigma_k))(\partial k/\partial y)]$, are compared in Fig. 4 under various Ar_b. The figures show that the model,

Table 2
The exact, modeled and expanded form of the k equation

	Exact form	Modeled form	Expanded form[a]
Turbulence diffusion + pressure diffusion + viscous diffusion	$\frac{\partial}{\partial x_j}\left(-\frac{\overline{u_i u_i u_j}}{2}\right) + \frac{1}{\rho}\frac{\partial \overline{pu_j}}{\partial x_j} + \frac{\partial}{\partial x_j}\left(\nu\frac{\partial k}{\partial x_j}\right)$	$\frac{\partial}{\partial x_j}\left[\left(\nu + \frac{\nu_t}{\sigma_k}\right)\frac{\partial k}{\partial x_j}\right]$	$\frac{\partial}{\partial y}\left[\left(\nu + \frac{\nu_t}{\sigma_k}\right)\frac{\partial k}{\partial y}\right]$
Shear production	$-\overline{u_i u_j}\frac{\partial U_i}{\partial x_j}$	$\nu_t\left(\frac{\partial U_i}{\partial x_j} + \frac{\partial U_j}{\partial x_i}\right)\frac{\partial U_i}{\partial x_j}$	$\nu_t\left(\frac{\partial U}{\partial y}\right)^2$
Gravity production	$-\beta g_i \overline{u_i t}$	$\beta g_i \frac{\nu_t}{Pr_t}\frac{\partial T}{\partial x_i}$	0
Dissipation	$\nu\overline{\frac{\partial u_i}{\partial x_j}\frac{\partial u_i}{\partial x_j}}$	$\frac{k^{3/2}}{l_\varepsilon}$	$\frac{k^{3/2}}{l_\varepsilon}$

[a] This column represents the results of applying eddy-viscosity model Eqs. (8)–(10) and the flow condition, Eq. (12), to the exact k-equation.

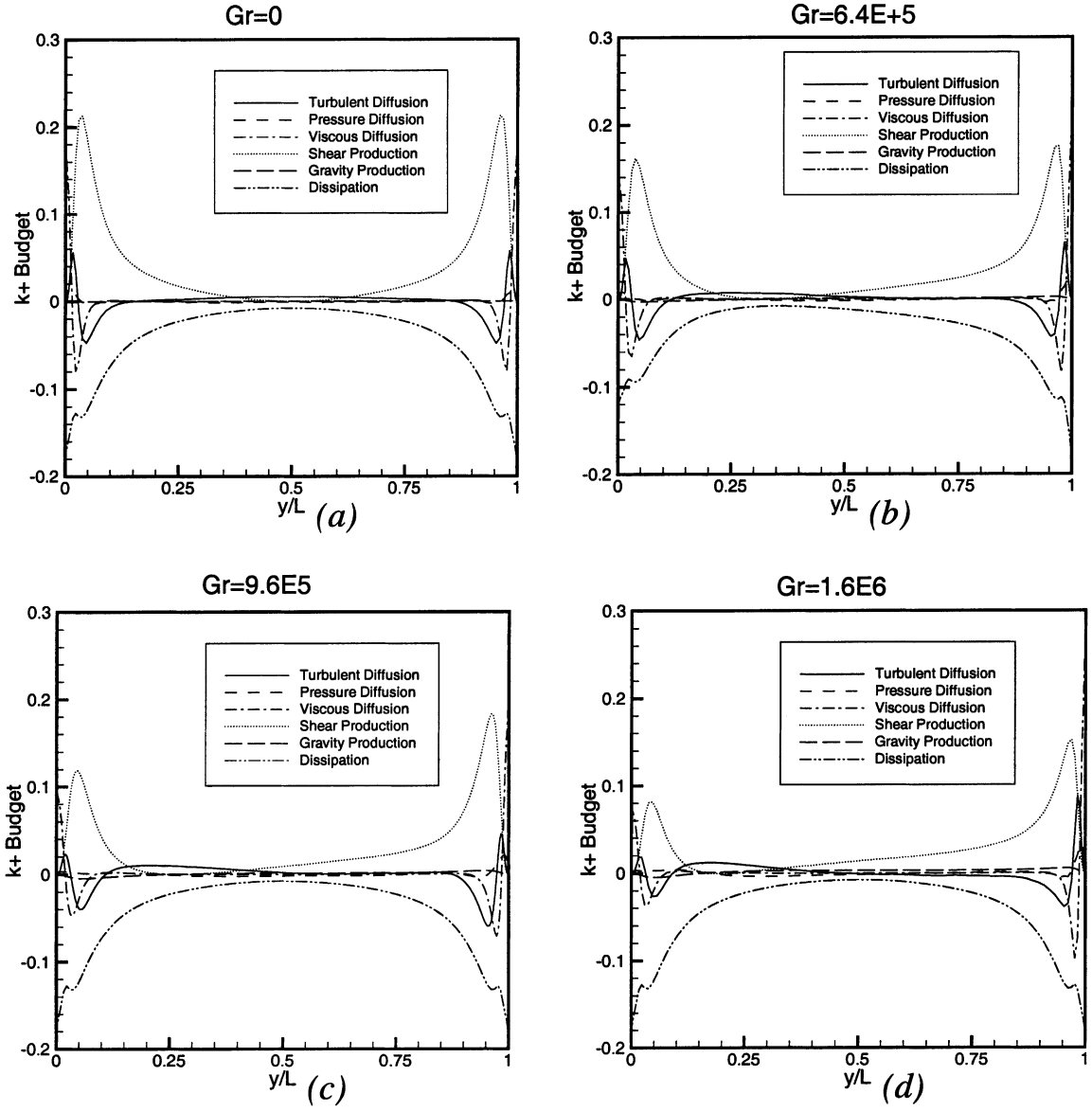

Fig. 2. k-Equation budget for cases 1–4. (a) $Re = 4350$, $Gr = 0.0$; (b) $Re = 4341$, $Gr = 6.4 \times 10^5$; (c) $Re = 4494$, $Gr = 9.6 \times 10^5$; (d) $Re = 4148$, $Gr = 1.6 \times 10^6$.

$(\partial/\partial y)[(\nu + (\nu_t/\sigma_k))(\partial k/\partial y)]$, describes the diffusion term very well under various Ar_b.

Fig. 5 illustrates that the second term, P_k, can be well represented by its model, $(\nu_t(\partial U/\partial y)^2)$, under all Ar_b. The counter-diffusion phenomena (which can be discerned by the negative value of P_k) found in the natural convection case [2] has not been observed in cases 1–4.

The third term, the gravity production, disappears after modeling due to the use of the eddy-viscosity assumption, Eq. (9), for turbulent heat flux. However, the energy budget (see Fig. 2) indicates that gravity production has a minor contribution to the total energy balance. Therefore, Eq. (9) remains a good approximation. Eq. (9) can also be used to determine the turbulent Prandtl number. Fig. 6a shows the Pr_t computed by $Pr_t = \nu_t(dT/dy)/(-\overline{vt})$ from the DNS cases 1–4. The figure suggests that Pr_t varies between 0.8–1 in most of the flow region. The commonly used value, 0.9, can be identified as a good approximation and therefore be used in the present study.

The last term, ε, has been shown in Fig. 6b. The figure shows that the trend of ε's variations with increases of Ar_b is similar to that of k. To calculate this term accurately, the length scale l_ε needs to be proposed properly. The length scale l_ε will be discussed in Section 2.3.

The term-by-term assessment indicates that the k-equation model describes the exact equation very well. However, it should be noted that the model assessment uses the ν_t derived from Kasagi and Nishimura's DNS data. Since one-equation models calculate ν_t by $C_\mu\sqrt{k}l_\mu$ or $\sqrt{\overline{vv}}l_\mu$, the prescription for the length scale l_μ is needed. In addition,

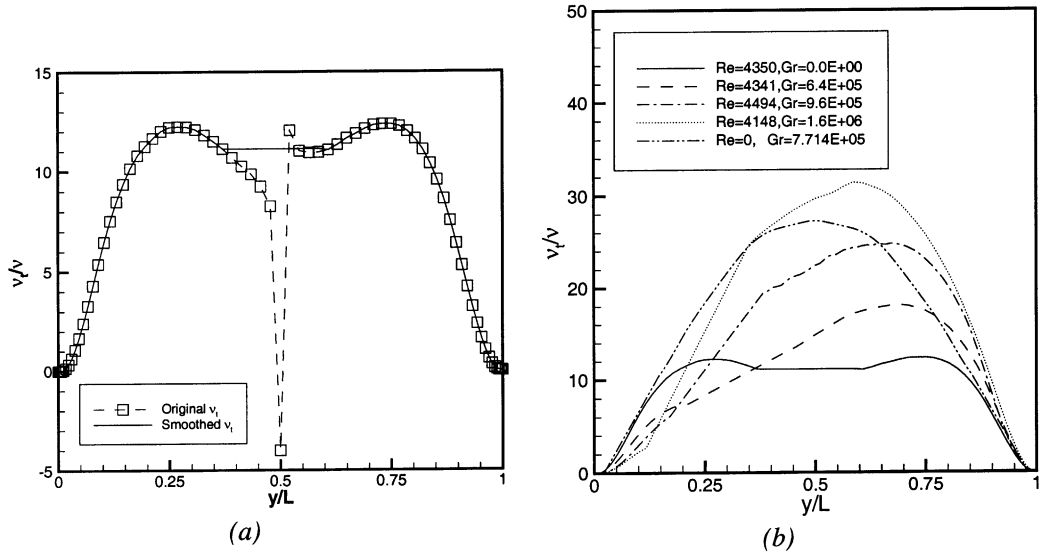

Fig. 3. Modeling v_t: (a) the v_t calculated by Eq. (13) and the smoothed v_t; (b) smoothed v_t of cases 1–5.

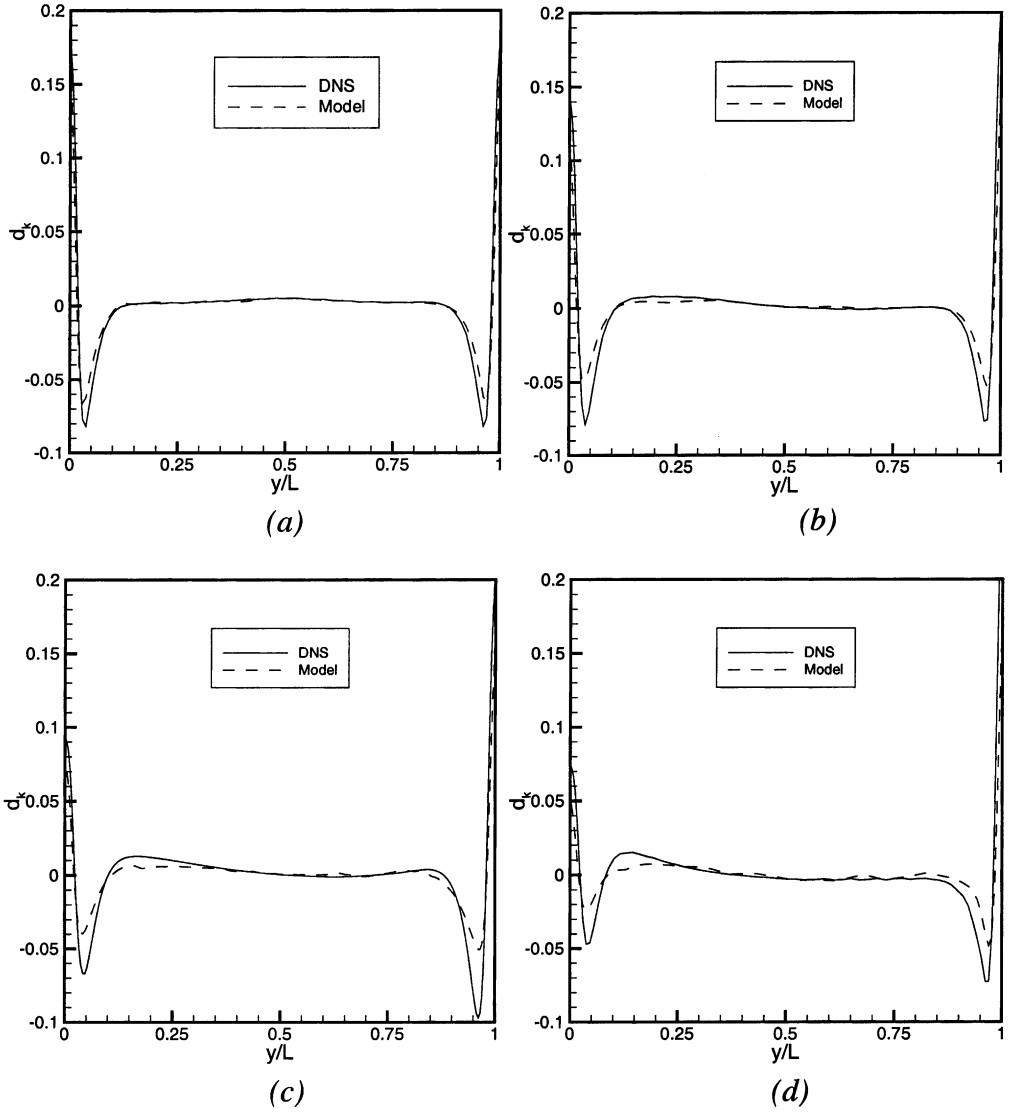

Fig. 4. The diffusion term d_k and its model for cases 1–4. (a) $Re = 4350$, $Gr = 0.0$; (b) $Re = 4341$, $Gr = 6.4 \times 10^5$; (c) $Re = 4494$, $Gr = 9.6 \times 10^5$; (d) $Re = 4148$, $Gr = 1.6 \times 10^6$.

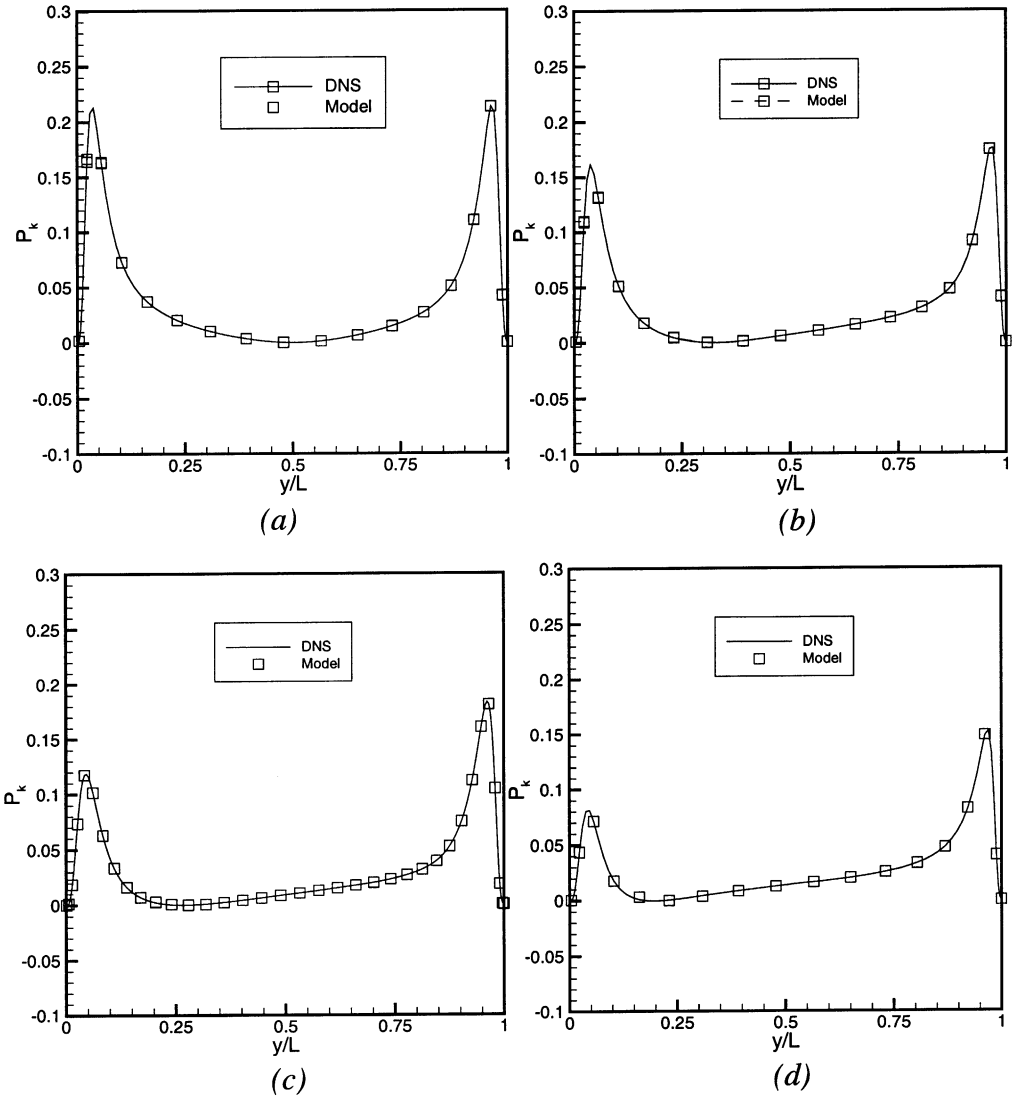

Fig. 5. The production term P_k and its model for cases 1–4. (a) $Re = 4350$, $Gr = 0.0$; (b) $Re = 4341$, $Gr = 6.4 \times 10^5$; (c) $Re = 4494$, $Gr = 9.6 \times 10^5$; (d) $Re = 4148$, $Gr = 1.6 \times 10^6$.

the dissipation term, ε, also requires prescribing a length scale l_ε Therefore, the prescriptions of the length scale l_μ and l_ε are very crucial to the accuracy of a one-equation model.

Xu et al. [2] suggested that the existing length-scale models, including Van Driest's [7] damping law, Norris and Reynolds' model [20] and Rodi's model [1], etc., fail to reproduce the DNS data of the natural convection case. The model developed by Xu et al. [2] can predict natural convection properly but may not be appropriate for forced or mixed convection. A new near-wall model that for various flow conditions is therefore need. The next section will show the model development.

2.3. A new one-equation turbulence model for near-wall flows

Forced and natural convection can be viewed as two extreme cases of mixed convection. With the increase of buoyancy, the flows transform from forced convection to natural convection. A model that can predict the flow under various buoyancy conditions must be able to correctly reproduce the two extreme cases and make a smooth transformation between them. To develop such a model, we proceed as follows. First, find two turbulence models appropriate for the two extreme cases: purely forced and purely natural convection. Second, find a parameter that can *scale* the buoyancy effects properly. Third, find a function that can gradually transfer turbulence models from one extreme case to the other according to the parameter found in the second step.

The first step requires identifying two turbulence models that are proper for purely forced and natural convection flows respectively. The model developed by Xu et al. [2] is a good candidate for the natural convection model. For the forced convection model, we have selected the one proposed by Rodi et al. [1], since the model has a structure similar to

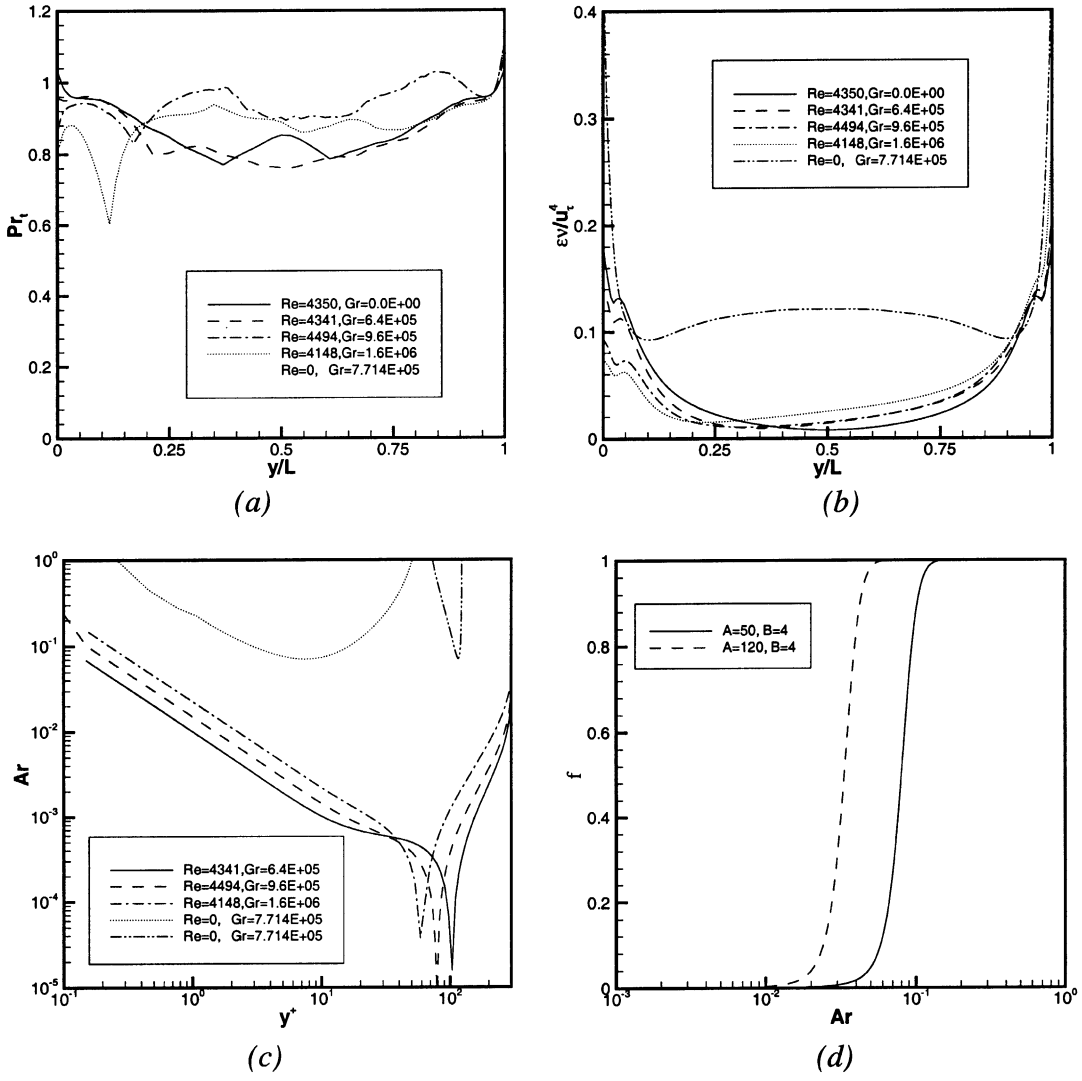

Fig. 6. (a) The turbulent Prandtl number for cases 1–4; (b) the diffusion term ϵ for cases 1–5; (c) $|Ar_y|$ for cases 1–5; (d) the transform function f, Eq. (28).

the natural convection model. For example, both models calculate the eddy viscosity by

$$v_t = \sqrt{\overline{vv}}\, l_\mu \tag{14}$$

and the dissipation by

$$\varepsilon = \frac{\sqrt{\overline{vv}}\, k}{l_\varepsilon} \tag{15}$$

and both use an algebraic equation to calculate $\overline{vv}/k$. Both models solve Eq. (1) in the nearwall region prescribe the length scales l_μ and l_ε and the correlation between the wall-normal-stress. The only difference is the prescriptions of the length scale.

For a smoother and easier transformation between the two models, we have slightly modified the forms of both models without significantly changing the values of the formulae. Tables 3 and 4 summarize the original and modified forms of the two models.

The second step is to find a parameter that can properly describe the relative importance of buoyancy and inertia in air. A natural selection of the parameter is the global Archimedes number, Ar_b, which is the ratio of global buoyancy force over inertia force. However, this global number is somewhat difficult to specify in a complex airflow since the selection of the characteristic parameters can be empirical. An alternative is the ratio of gravity production over shear production. But Table 2 shows that the *model* of gravity production goes to zero in some cases while the actual production does not. This indicates that the selection of the ratio will require more efforts on the turbulence modeling of the gravity production term. Therefore, we have chosen a simple parameter, the local Archimedes number. The local Archimedes number can be defined as

$$Ar_l = \frac{g\beta\Delta T l}{U^2} \tag{26}$$

Table 3
The original and modified forms of the natural convection model

	Original form		Modified form
l_μ	$l_\mu = \dfrac{0.544y}{1 + 5.025 \times 10^{-4} y_v^{*1.65}}$	(16)	Same
l_ε	$l_\varepsilon = \dfrac{8.8y_n}{1 + 10/y_v^* + 5.15 \times 10^{-2} y_v^*}$	(17)	Same
$\dfrac{\overline{vv}}{k}$	$\dfrac{\overline{vv}}{k} = 7.19 \times 10^{-3} y^* - 4.33 \times 10^{-5} y^{*2} + 8.8 \times 10^{-8} y^{*3}$	(18)	$\dfrac{\overline{vv}}{k} = 0.4\left[1 - \exp\left(-\dfrac{y^*}{42}\right)\right]$

Table 4
The original and modified forms of the forced convection model

	Original form		Modified form	
l_μ	$l_\mu = 0.33y_n$	(20)	$l_\mu = \dfrac{0.33y}{1 + 5.025 \times 10^{-4} y_v^{*1.53}}$	(23)
l_ε	$l_\varepsilon = \dfrac{1.3y_n}{1 + 2.12/y_v^*}$	(21)	$l_\varepsilon = \dfrac{1.3y_n}{1 + 2.12/y_v^* + 2.8 \times 10^{-2} y_v^*}$	(24)
$\dfrac{\overline{vv}}{k}$	$\dfrac{\overline{vv}}{k} = 4.00 \times 10^{-4} y^* + 4.65 \times 10^{-5} y^{*2}$	(22)	$\dfrac{\overline{vv}}{k} = 0.4\left[1 - \exp\left(-\dfrac{y^{*2}}{4200}\right)\right]$	(25)

where ΔT is the difference between the local and reference temperature and U is the local velocity. Since the parameter is primarily used in a near-wall model, the wall-distance, y_n, is chosen for the length scale l in Eq. (26), so

$$Ar_y = \frac{g\beta\Delta T y_n}{U^2} \tag{27}$$

Obviously, Ar_y is positive in aiding flows and negative in opposing flows. Fig. 6c plots the $|Ar_y|$ with respect to the y^+ for the cases 1–5. Ar_y systematically changes with Ar_b. The natural convection case has the largest values of Ar_y.[1] This suggests that Ar_y is a good indicator of the buoyancy effects.

The last step in the model development is to find a function that can smoothly transfer one model to the other according to Ar_y. The function should vary from 0 to 1 smoothly and be stable for all possible Ar_y. The following function is acceptable for both requirements:

$$f = \tfrac{1}{2}[1 + \tanh(A|Ar_y| - B)] \tag{28}$$

where A and B are constants to control slope and location of the transition point. Eq. (28) shows that $f = 0$ when $Ar_y = 0$ and $f \to 1$ when $Ar_y \to \pm\infty$. After a trial-and-error process, we obtain $A = 50$, $B = 4$ for calculating l_μ and l_ε, $A = 120$, $B = 4$ for calculating $\overline{vv}/k$. According to Fig. 6c, the Ar_y for natural convection is well above 0.1. The two sets of constants give the transformation points at $|Ar_y| = 0.08$ for l_μ and l_ε and 0.033 for $(\overline{vv}/k)$, respectively, which means when $|Ar_y| > 0.08$ or 0.033, $f > 0$. Fig. 6d shows the curve described by Eq. (28) with the two sets of constants.

It should be noted that Eq. (28) uses $|Ar_y|$ instead of Ar_y. The reason is that in a natural convection case, the length scales on heated and cooled sides are the same so that Eq. (28) can be used. In a mixed convection case, the heated and cooled sides are different only under very small Ar_b. The length scales for aiding and opposing flows behave similarly and approach the same with an increase of Ar_b. Secondly, a transform function that can account for the small differences between aiding and opposing flows requires more DNS databases or experimental data to determine the complex shape of the function. In addition, the transform function f described in Eq. (28) is mathematically simple and stable. After all, all the transform functions and length-scale prescriptions can be verified only through examining their performance in practical applications.

With the scale parameter Ar_y and transform function Eq. (28), the final form of the new model can be written as follows:

$$l_\mu = \frac{(0.33 + 0.214 f_{l_\mu})y}{1 + 5.025 \times 10^{-4} y_v^{*[1.53 + 0.12 f_{l_\mu}]}} \tag{29}$$

$$l_\varepsilon = \frac{(1.3 + 7.5 f_{l_\varepsilon})y}{1 + (2.12 + 7.88 f_{l_\varepsilon})/y_v^* + (0.028 + 0.0235 f_{l_\varepsilon}) y_v^*} \tag{30}$$

$$\frac{\overline{vv}}{k} = 0.4\left[1 - \exp\left(-\frac{y^{*(2 - f_{vv/k})}}{4200(1 - 0.99 f_{vv/k})}\right)\right] \tag{31}$$

where

$$f_{l_\mu} = f_{l_\varepsilon} = \tfrac{1}{2}[1 + \tanh(50|Ar_y| - 4)] \tag{32}$$

$$f_{vv/k} = \tfrac{1}{2}[1 + \tanh(120|Ar_y| - 4)] \tag{33}$$

[1] The velocity at the centerline is zero in the natural convection case. This contributes to the steep increase of the dobule-dotted dashed line, which corresponds to the natural convection case.

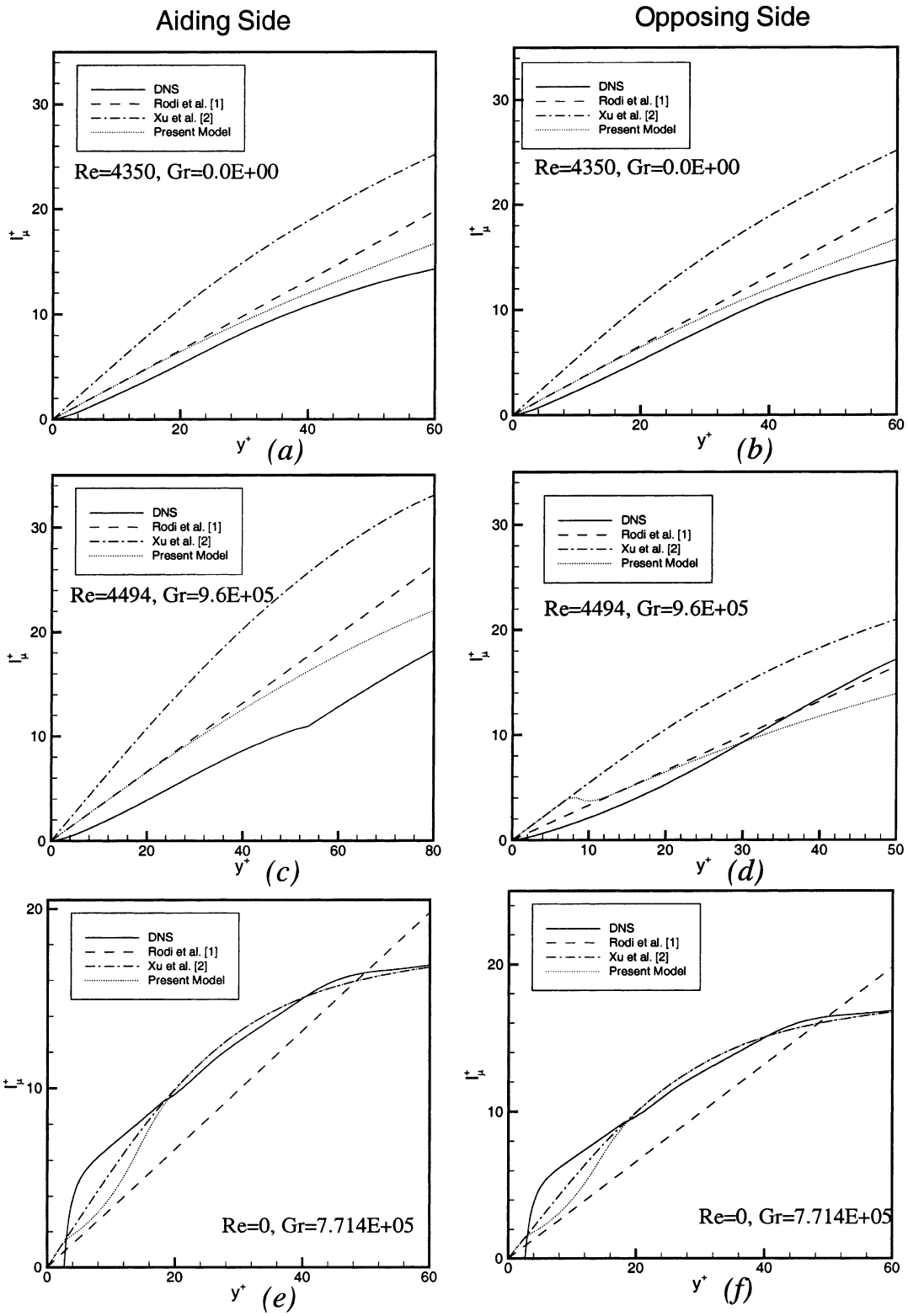

Fig. 7. Comparison of l_μ for cases 1, 3 and 5; (a), (c), (e): aiding side; (b), (d), (f): opposing side.

Figs. 7–9 show the curves calculated by Eqs. (29)–(31) and compare them with Rodi's [1] model and the Xu's [2] model for the DNS cases 1, 3 and 5, which correspond to the forced, mixed and natural convection cases. The figures show that Rodi's model, which was developed for isothermal flows, agrees with the mixed convection case better than Xu's natural convection model. This is because the DNS results contain only weak buoyancy and the flow characteristics are

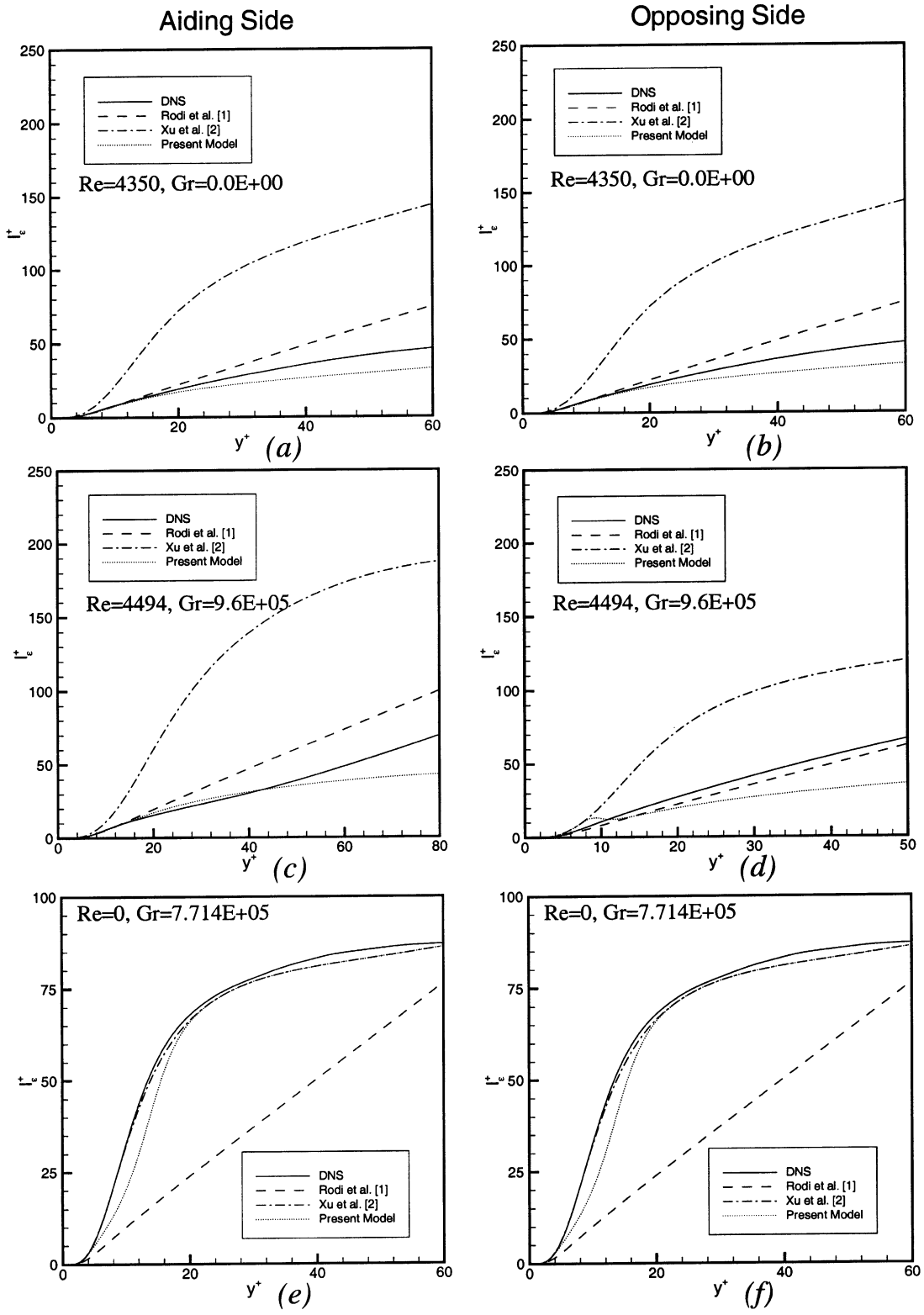

Fig. 8. Comparison of l_ε for cases 1,3 and 5; (a), (c), (e): aiding side; (b), (d), (f): opposing side.

similar to those of isothermal flows. However, Rodi's model fails in the natural convection case, as shown in Figs. 7e, 7f, 8e and 8f. On the other hand, Xu's model is superior in the natural convection case but not in the forced and mixed convection cases. In contrast, Figs. 7 and 8 show that the l_μ and l_ε calculated by Eqs. (29) and (30) perform universally well. Fig. 9d shows a small 'step' in the predicted curve. The step occurs only in a small range $y^+ = 10$–14, which

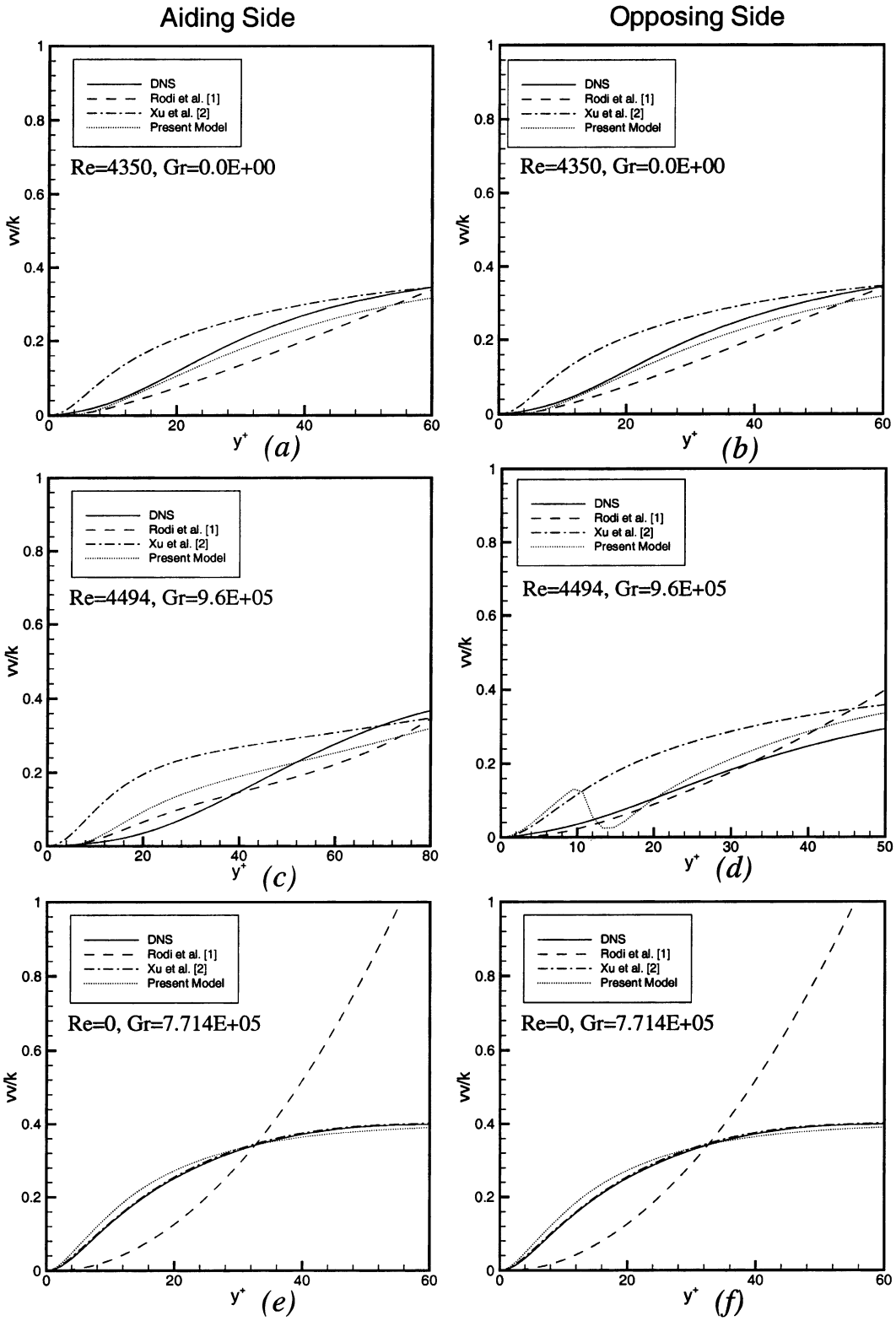

Fig. 9. Comparison of vv/k for cases 1, 3 and 5; (a), (c), (e): aiding side; (b), (d), (f): opposing side.

indicates that the model successfully transforms. After the transformation, the curve agrees with the DNS data well. Other figures in Fig. 9 show that very good agreement occurs between Eq. (31) and the DNS data.

2.4. A two-layer model

A two-layer model can be formed with the model developed in Section 2.3 and the standard k–ε model. The newly

developed model will be used in the near-wall region and the standard k–ε model will be used in the outer-wall region. The model switching procedure is the y^*-prescription method, which switches the two models according to the local y^* value, i.e. if $y^* < y^*_{\text{prescribed}}$ the new model applies; otherwise, the standard k–ε model will be used. Since the new model is expected to be used universally, the switch value of y^* should be approximately equal to $\min(y^*_{\text{natural}}, y^*_{\text{forced}})$. Xu et al. [2] set the switching y^* to 160 for the natural convection case. The forced convection model can be used within $y^* < 60$ (Rodi et. al. [1]). We therefore compromise two criteria and empirically set the switching criterion as $y^* = 80$.

The implementation of the new two-layer model with y^* prescription method can be summarized as follows:

1. In the near-wall region, where $y^* < 80$, the new one equation model is used; i.e. the k is solved by Eq. (1), i.e.

   $$\frac{\partial k}{\partial t} + U_i \frac{\partial k}{\partial x_i} = d_k + P_k + G_k - \varepsilon$$

   the eddy viscosity is calculated by, $\nu_t = \sqrt{\overline{vv}}\, l_\mu$; the ε by $\varepsilon = (\sqrt{\overline{vv}}\, k / l_\varepsilon)$ and l_μ, l_ε, and $(\overline{vv}/k)$ by Eqs. (29)–(31), respectively.
2. In the outer-wall region, where $y^* \geq 80$, the standard k–ε model [21]. The eddy viscosity is calculated by $\nu_t = C_\mu (k^2/\varepsilon)$, where $C_\mu = 0.09$. No length scale prescription is needed.

3. Conclusions

With the aid of the DNS data [3], this paper has developed a two-layer near-wall turbulence model for indoor aifflow simulation. The model combined the two-layer models from Rodi et al. [1] and Xu et al [2]. A scaling parameter Ar_y and a transform function have been used to consider the variation of buoyancy effects in the model. The model is capable to predict forced, natural and mixed convection airflow indoors.

Acknowledgements

This study is supported by the National Science Foundations through grant CMS-9623864.

References

[1] W. Rodi, N.N. Mansour, V. Michelassi, One-equation near-wall turbulence modeling with the aid of direct simulation data, Journal of Fluid Engineering 115 (1993) 196–205.

[2] W. Xu, Q. Chen, F.T.M. Nieuwstadt, A new turbulence model for near-wall natural convection, International Journal of Heat Mass Transfer 41 (1998) 3161–3176.

[3] N. Kasagi, M. Nishimura, Direct numerical simulation of combined forced and natural convection in a vertical plane channel, International Journal of Heat and Fluid Flow 18 (1997) 88–99.

[4] M. Nakajima, K. Fukui, Buoyancy effects on turbulent transport in combined free and forced convection between vertical parallel plates, International Journal of Heat Mass Transfer 23 (10) (1980) 1325–1336.

[5] T.S. Chen, B.F. Armaly, M.M. Ali, Turbulent mixed convection along a vertical plate, Journal of Heat Transfer 109 (1987) 251–253.

[6] T. Aicher, H. Martin, New correlations for mixed turbulent natural and forced convection heat transfer in vertical tubes, International Journal of Heat Mass Transfer 40 (15) (1997) 3617–3626.

[7] E.R. Van Driest, On turbulent flow near a wall, Journal of Aeronautical Science 23 (1956) 1007.

[8] H. Schwenke, Ueber das Verhalten elener horizontaler Zuluftstrahlen im begrenzten Raum, Luft- und Kaltetechnik 5 (1975) 241–246.

[9] D. Blay, S. Mergui, C. Niculae, Confined turbulent mixed convection in the presence of a horizontal buoyant wall jet, Fundamentals of Mixed Convection, HTD 213 (1992) 65–72.

[10] P.V. Nielsen, A. Restivo, J.H. Whitelaw, Buoyancy-affected flows in ventilated rooms, Numerical Heat Transfer 2 (1979) 115–127.

[11] J.D. Jackson, M.A. Cotton, L.S.L. Yu, M.M. Rouai, Experimental and computational studies of turbulent forced and mixed convection heat transfer to water in a vertical pipe, in: W. Rodi, E.N. Ganic (Eds.), Engineering Turbulence Modeling and Experiments, Elsevier, New York, 1990, pp. 809–818.

[12] T. Inagaki, K. Komori, Numerical modeling on turbulent transport with combined forced and natural convection between two vertical parallel plates, Numerical Heat Transfer 27 (part A) (1995) 417–431.

[13] G.A. Fedorov, R. Viskanta, A.A. Mohamad, Turbulent heat and mass transfer in an asymmetrically heated vertical parallel-plate channel, International Journal of Heat and Fluid Flow 18 (1997) 307–315.

[14] K. Patel, B.F. Armaly, T.S. Chen, Transition from turbulent natural to turbulent forced convection adjacent to an isothermal vertical plate, HTD 324 (1996) 51–56.

[15] W.M. To, J.A.C. Humphrey, Numerical simulation of turbulent buoyancy, turbulent flow — I. Free convection along a heated, vertical, flat plate, International Journal of Heat Mass Transfer 29 (1986) 573–592.

[16] Q. Chen, Comparison of different k–ε models for indoor air flow computations, Numerical Heat Transfer (part B) 28 (1995) 353–369.

[17] Q. Chen, Prediction of room air motion by Reynolds-stress models, Building and Environment 31 (1996) 233–244.

[18] T.A.M. Versteegh, F.T.M. Nieuwstadt, Scaling of free convection between two differentially heated infinite vertical plates, Turbulent Shear Flow 11 (1996).

[19] L. Prandtl, Uber ein Neues Formelsystem fur die ausgebildete Tirbulenz, Nacr. Akad. Wiss. Gottinggen Math-Phys. Kl. 6 (1945) 19.

[20] L.H. Norris, W.C. Reynolds, Turbulent channel flow with a moving wavy boundary, Report number FM-1O, Department of Mechanical Engineering, Stanford University, 1975.

[21] B.E. Launder, D.B. Spalding, The numerical computation of turbulent flows, Computer Methods in Applied Mechanics and Energy 3 (1974) 269–289.